scientific reports

Check for updates

OPEN

Analysis of the influence of coupling agents on the composition of artificial rocks with polymer matrix

Marcelo Barcellos Reis[1], Elaine Aparecida Santos Carvalho[1], Geovana Carla Girondi Delaqua[1], Afonso Rangel Garcez de Azevedo[2]✉, Sérgio Neves Monteiro[3] & Carlos Maurício Fontes Vieira[1]

While advances in material improvement are significant, actual adoption still depends on balancing cost, environmental impact, and performance. High-specification chemicals and complex processes can increase production costs, and the sustainability of new, partially synthetic systems must be examined. In this context, this study explored an alternative approach for agglomerated rocks, where the use of coupling agents enhances interface engineering. We addressed the mineral-polymer relationship by comparing two epoxy resins and two polyester resins with and without silane-based coupling agents (γ-APS for epoxies; MPTS for polyesters) in 85% by weight of granite waste. Original contributions include: a mix design selection (simplex network) for the densest packing (grain size: 66% coarse, 17% medium, 17% fine) by vibrated bulk density, validated via ANOVA/Tukey; a unified manufacturing route using vibropressing, vacuum compaction, and vacuum hot pressing (600 mmHg, 10 MPa, 90 °C). Physical indices (bulk density, open porosity, and water absorption) were evaluated in accordance with ABNT NBR 15845-2. Three-point bending tests were performed using ABNT NBR 15845-6 (for slabs) and ASTM D790 (for neat resins). Thermal behavior and fracture micromechanics were assessed through TGA/DSC (ASTM D6370) and SEM. Silanes increased bulk density and drastically reduced porosity and water absorption (by 61% and 84%, respectively), while increasing flexural strength by 16–38% in all resin families; neat epoxy with γ-APS also showed substantial strengthening. TGA indicated a higher onset of degradation and lower mass loss; SEM showed more cohesive fracture, consistent with siloxane anchoring to silicates and amine-epoxy or thiol-ene reactions. By combining particle packing optimization with targeted interfacial chemistry at moderate processing temperatures, the approach confirms the goals of agglomerated rock, such as improved qualities while mitigating the costs and environmental impacts associated with conventional designs that require higher resin percentages.

Keywords Coupling agents, Artificial rock, Polyester resin, Epoxy resin

Brazil today is ranked as the 5th largest exporter of ornamental stones (below only China, India, Turkey, and Italy) in the world[1]. The geological diversity (mainly in quartzites and exotic granites) of Brazil is the reason for its competitiveness and is different from that of other countries in the world.

The importance of artificial rocks in Brazil has been growing since 2019. In 2024, imports amounted to US$12.4 million (20.4 thousand tons) in the 1 st quarter, and Turkey, Mexico, Egypt, and Italy were the leading suppliers[2]. This increase in imports is due to the search for new types of materials, with specific characteristics that are difficult to find in the country's natural stones, such as homogeneity (in color) and resistance (mechanical).

The Brazilian Natural Rocks Association[2] reports that in 2014, the Brazilian ornamental rock market recovered significantly and consolidated itself as one of the world's leading exporters. The result of Brazilian exports in 2024 was US$1.263 billion, representing a 12.7% increase compared to the previous year. Although

[1]Advanced Materials Laboratory (LAMAV), State University of Norte Fluminense (UENF), Av. Alberto Lamego, Campos dos Goytacazes, Rio de Janeiro 2000, CEP 28013-602, RJ, Brazil. [2]Civil Engineering Laboratory (LECIV), State University of Norte Fluminense-UENF, Av. Alberto Lamego 2000, Campos dos Goytacazes, 28013-602, RJRio de Janeiro, Brazil. [3]Department of Materials Science, Military Institute of Engineering (IME), Praça General Tibúrcio, 80, Praia Vermelha, Urca, Rio de Janeiro CEP 22290-270, RJ, Brazil. ✉email: afonso@uenf.br

the economic return of these values has a positive impact, the environmental implications are negative due to the enormous amount of solid waste generated by this industrial process.

An alternative to reducing waste from the production of ornamental rocks is the manufacture of artificial rocks, also known as synthetic rocks, which are produced from high levels of solid particles, approximately 85% of which is solid waste, commonly originating from the processing stages of ornamental rocks. These particles can be artificial by two types of matrices, polymeric and cementitious[3].

The application of artificial rocks generally presents several advantages over ornamental rocks, with a particular emphasis on polymeric matrix rocks, which typically have lower density and fewer pores, resulting in improved material performance and reduced risk of crack formation, for example. Another significant advantage concerns physical performance, mechanical, thermal, and chemical, given the efficiency of the interaction of the mineral filler with the polymeric matrix[4,5].

The production of artificial rocks is more ecologically viable than ornamental rocks, as they generate a smaller amount of polluting gases during processing and require less energy to create the product[6,7]. Another advantage is the use of waste and the circular economy, as the incorporation of by-products such as granite dust, foundry sand, and fly ash, not only diverts these materials from landfills, but also adds value to flows that would be considered "waste" by the industry, promoting the circular economy and avoiding disposal impacts[8].

The fabrication of polymer matrix artificial rocks includes a massive range of materials in its composition. In addition, it involves scientific research associated with the potentialization of results, concept improvement, and testing new chemical agents and reagents[9,10].

Coupling agents are an essential tool in this process because they work by adhering both the particulate material reinforcement and the polymer matrix through chemical bonds or chain entanglement. This dual 'adhesion capability is essential to improve the mechanical properties of composites by reducing interfacial tension and improving phase adhesion between immiscible polymers[11,12].

The production of artificial rocks is more ecologically viable than ornamental rocks, as they generate a smaller amount of polluting gases during processing and require less energy to create the product[6,7]. Another advantage is the use of waste and the circular economy, as the incorporation of by-products such as granite dust, foundry sand, and fly ash, not only diverts these materials from landfills, but also adds value to flows that would be considered "waste" by the industry, promoting the circular economy and avoiding disposal impacts[8].

The fabrication of polymer matrix artificial rocks includes a massive range of materials in its composition. In addition, it involves scientific research associated with the potentialization of results, concept improvement, and testing new chemical agents and reagents[9,10].

Coupling agents are an essential tool in this process because they work by adhering both the particulate material reinforcement and the polymer matrix through chemical bonds or chain entanglement. This dual 'adhesion capability is essential to improve the mechanical properties of composites by reducing interfacial tension and improving phase adhesion between immiscible polymers[11,12].

Silanes have a general structure represented by $R–Si(OR')_3$, in which R is an organic functional group such as vinyl, amino, epoxy, or methacryloxy, compatible with polymer resins like epoxy and polyester. OR' is an alkoxy group, usually methoxy or ethoxy, responsible for the reaction with the inorganic surfaces of minerals. Changes in chemical bonds at the interface occur on the surface of the mineral fillers' inorganic phase, through hydrolysis or condensation, causing a transition from the originally polar (hydrophilic) surface to a surface more compatible with the organic matrix (hydrophobic). By hydrolysis, the alkoxy groups (–OR') of the silane undergo reactions in the presence of moisture, forming silanol groups (–Si–OH). By condensation with the mineral filler, the silanol groups react with free hydroxyl groups on the mineral surface, creating strong covalent bonds (Si–O–Si), fixing the silane to the mineral filler[13].

Changes in chemical bonds also occur at the silane-resin interface [organic phase]. In chemical reactions with the resin, the organic functional group (R) of the silane reacts by covalent bonding with the active groups of the resin. For epoxy resins, silanes with amine or epoxy groups are usually used, which react directly with the epoxy groups of the resin using an oxirane ring-opening reaction, forming stable covalent bonds. For polyester resins, silanes with vinyl or methacryloxy groups are frequently used, which react using radical polymerization during the curing of the polyester resin, resulting in covalent bonds with the polymer matrix[14].

The silane coupling agents recommended in this research have a wide range of applications in composites, increasing the bond strength between inorganic fillers and organic polymers. These agents have functional groups capable of binding to both surfaces, making them versatile for various applications. They play a key role in surface modification to improve the mechanical properties, durability, and overall performance of composites[15].

Li et al.[16], used dual silane coupling agents in a formulation combining quartz powder and epoxy resin, resulting in a significant improvement in the composite properties. The composite showed a 16.89% increase in flexural strength and a 30.01% increase in tensile strength. Additionally, another study examined the effect of various silane coupling agents on enhancing the efficiency of carbon fiber and polymer composite properties. This research led to improvements in tensile properties, thermal properties, and surface interface characteristics[17].

The present research work aims to analyze the potential use of silane coupling agents in the composition of artificial rocks with granite mineral filler in a polymeric matrix, thereby optimizing their properties compared to those of ornamental rocks. For this purpose, two types of epoxy resin, two types of polyester resin, and two types of coupling agents were used, as listed in the following reaction.

Materials and methods

Materials

The black granite ornamental rock waste, marketed under the name of São Gabriel, was purchased from Ribertex Chemical Specialties LTDA (Belo Horizonte/Brazil), with the following particle sizes: coarse (16–40 mesh), medium (40–200 mesh), and fine (200–250 mesh). Four types of resins commercially available from Redeleaser

resin	model	complement	hardener/catalyst	proportion [g]	manufacturer
epoxy	4008	low viscosity	5000	100:43	Redeleaser
epoxy	MC130	high viscosity	FD129	100:10	Epoxyfiber
polyester	orthophytal	low viscosity	M50	100:1	Redeleaser
polyester	isophthalic	low viscosity	M50	100:1	Redeleaser

Table 1. Types of resins.

model	chemical name	type of resin	manufacturer
Silano 172	3-Mercaptopropyltiethoxysilane	polyester	Ecopower Chemical Co. Limited
Silano 1100	γ–Aminopropiltrietoxilsilane	epoxy	Ecopower Chemical Co. Limited

Table 2. Types of coupling agents.

Class	Sieve [Mesh #]	Granulometric Range [mm]
Coarse	16–40	2.000–0.420
Medium	40–200	0.420–0.075
Fine	200–250	0.075–0.063

Table 3. – Granulometric compositions.

and Epoxyfiber were used in this study: two types of epoxy and two kinds of polyester, listed in Table 1, both with their respective hardeners and catalysts.

The silane coupling agents were purchased from Delquímica Commercial LTDA, São Paulo/Brazil. Their information is detailed in Table 2.

parameters for characterization of granite residue

The chemical characterization of the black granite residue was performed by X-ray fluorescence (XRF) using a model ZSX PRIMUS II RIGAKU spectrometer, following the B100-PR CR 098 method[18]. XRF is a semi-quantitative chemical analysis that provides the percentages of the elemental composition of the inorganic constituents present in the material's structure. The mineralogical characterization of the black granite residue was performed by X-ray diffraction (XRD) using a PROTO AXRD diffractometer with monochromatic Cu K-$\boldsymbol{\alpha}$ radiation and a speed of 1.5° (2$\boldsymbol{\theta}$) per min. This XRD reveals the types of minerals present in the black granite residue.

Development parameters of artificial rocks

The granulometric reduction of the black granite residue was confirmed by the acceptable sieving method according to ABNT NBR 7181[19] Table 3 establishes three granulometric ranges: coarse, medium, and fine particles.

The mixture of these particles aims to determine a granulometric profile of the sample, optimizing the packaging of its particles, and to identify the main ideal granulometric ranges of the residue for experimental work in manufacturing artificial rock. Using the three particle size ranges (coarse, medium, and fine), 10 mixtures of particles with different compositions were proposed based on the ternary diagram of the complete cubic model, as presented in the Simplex-Lattice Design (SLD) numerical modeling system in Fig. 1. In this diagram, each point represents a mixture of a given composition. The objective of these 10 mixtures was to obtain the one with the maximum dry density, consequently, better packaging. Each vertex of the triangle corresponds to 100%: coarse (G), medium (M), and fine (F) particles. The other points, in parentheses of the triangle, show the fractions corresponding to the mixtures. The density of each mixture was calculated according to the Brazilian standard[20].

Statistical treatments were performed on the results of the vibrated density test, using analysis of variance (ANOVA) of the completely randomized design [DIC] ($p < 0.05$), to confirm the statistical significance of the data obtained. After validating the statistical difference, the Tukey test ($p < 0.05$) was applied to corroborate the mixture that received the best results, chosen to produce the artificial rock slabs.

Factorial design is applied in several scientific studies. Javorsky et al.[21], used a complete factorial design to study the adhesion of polyvinyl chloride (PVC) to stainless steel for automotive applications. Romli et al.[22], used a complete factorial design with two levels for the curing time factor and three levels for the fiber volume and compressive load factors, in a study dealing with a fiber-reinforced epoxy composite.

Each mixture was packaged in a 1,013.24 cm^3 steel container coupled to a 10 kg weight, subjected to a vibration of 60 Hz for 10 min. Table 4 shows the vibration density of the 10 mixtures proposed in Fig. 1.

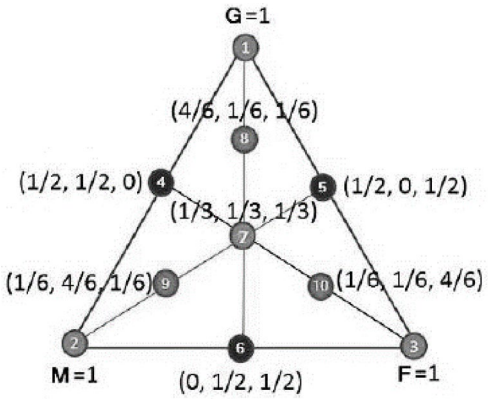

Fig. 1. Ternary diagram of the simplex centroid model.

# Mixture	Coarse [%]	Medium [%]	Fine [%]	Vibrated Density [g/cm^3]
1	1	0		1.8760 ± 0.0443
2	0	1	0	1.6580 ± 0.0384
3	0	0	1	1.4097 ± 0.0262
4	1/2	1/2	0	1.7904 ± 0.0141
5	1/2	0	1/2	1.4360 ± 0.2275
6	0	1/2	1/2	1.5659 ± 0.0565
7	1/3	1/3	1/3	1.5166 ± 0.0721
8	2/3	1/6	1/06	2.1097 ± 0.0047
9	1/6	2/3	1/6	1.8476 ± 0.0389
10	1/6	1/6	2/3	2.0139 ± 0.0162

Table 4. Vibrated density- 10 mixtures.

Source of Variation	Degrees of Freedom	Sum of Squares	Mean Square	Statistic F
Treatment	9.0000	3.9114	0.4346	41.0462
Residue	20.0000	0.2118	0.0106	
Total	29.0000	4.1231		

Table 5. ANOVA for DIC of vibrated density [$p \leq 0.05$]. Conclusion: Calculated F > tabulated F, indicating a statistically significant difference. Tabulated F = 2.39.

Through statistical analysis, where variance and multiple comparisons between means were examined, packaging #8, with a vibrated density of 2.1087 ± 0.0047 g/cm^3, yielded the best result (a more compacted mixture) and was chosen for this research work.

Table 5 presents the ANOVA for the vibrated density parameter, while Table 6 presents the Tukey test for the same parameter. For the ANOVA, three repetitions were used for each of the 10 mixtures.

Analyzing the results presented in Tables 5 and 6, it is evident that a statistical difference exists, indicating that at least four of the 10 mixtures are differentiated.

A fact that can change the packing condition is the morphology of the particles. The less spherical the particle, the lower the packing density of a distribution. The smaller the size of the irregular particles, the greater this effect will be, due to the greater specific surface area[23]. Barreto et al.[24] emphasize that the use of mixtures with greater packaging results in economic advantages, since the existence of lower porosity levels requires less use of resin for the production of rocks. A pycnometry test was also conducted to determine the actual density of the black granite residue, which was subsequently used to calculate the volume of voids and the minimum resin content required for producing artificial rock plates, as related to packaging #8.

Methods

To fabricate the artificial rocks, the void volume (VV) was initially calculated using:

$$VV\% = 1 - \left[\frac{\textbf{Dry apparent density of particles}}{\textbf{Residue Density}}\right] \text{x } 100 \quad (1)$$

treatment	average	Tukey's test
8	2.11	A
10	2.01	AB
1	1,88	AB
9	1,85	AB
2	1,66	BC
6	1.57	BC
7	1.52	CD
5	1.44	CD
3	1.41	CD
4	0.79	E

Table 6. Tukey test for contrast of vibrated density means.

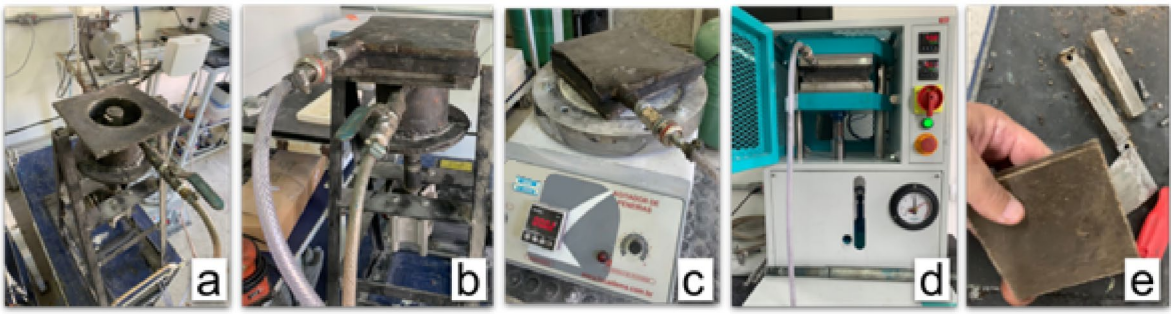

Fig. 2. Stages of manufacturing artificial rock slabs: [a] mixer; [b] vacuum molding in the mixer; [c] vacuum molding on the shaker; [d] vacuum compaction molding; [e] unmolded raw plate.

Where the dry bulk density of the particles refers to the average packing density, and the residue density is the average of the proper density.

The minimum amount of resin (MAR) required to fill the void volume for the manufacture of artificial rocks is presented below:

$$MAR\% = \frac{\mathbf{VV\%\ x\ \rho\ resin}}{(\mathbf{VV\%\ x\ \rho\ resin}) + [100 - \mathbf{VV\%}]\ \mathbf{x\ \rho\ residue}} x\ 100$$

Where ρ resin is the density of the resin and ρ residue is the density of the residue.

After determining VV and MAR, the value of 15% resin was obtained for the manufacture of artificial rock plates for the chosen packaging. The definition of this value considers the wettability in the waste/resin interaction process. In practice, a portion of the resin is lost when transferring it from the measuring container to the mixing system.

Development parameters of artificial rock plates

The black granite residue, as specified in the granulometries in Table 3, was dried in an oven at 100 °C for 24 h to remove moisture. Then, the chosen packaging, consisting of 2/3 coarse, 1/6 medium, and 1/6 fine, was weighed in the appropriate proportions and taken to the automatic cylindrical mixer, along with the resins listed in Fig. 2; Table 1, and their respective catalysts/hardeners in the proportions indicated by the manufacturers.

The process for preparing the mixtures was carried out for each type of resin. Sometimes, with the addition of the coupling agents, listed in Table 2, and sometimes without the addition of the coupling agents, so that the results of the proposed tests could be later compared.

As illustrated in Fig. 2(a), the mixture was then placed in a metal mold to produce plates measuring 100 × 100 × 10 mm, which were connected to a vacuum system (600 mmHg) and vibrated for 2 min [Figure 2(b)]. This step helps to remove air from the interstices of the grains, which promotes plasticity, thus facilitating resin wetting and better particle distribution[25].

The vibration stage is then performed for 2 min at 60 Hz, as shown in Fig. 2(c). The mold, still under vacuum for another 2 min, was positioned in a hydraulic press, where it was compressed (10 MPa) for 20 min at 90 °C, as shown in Fig. 2(d), to facilitate the curing of the resin[26].

After the compaction stage was completed, the slabs were demolded, Fig. 2(e), the burrs were removed and placed in an oven at 100 °C for 24 h, a stage that optimizes the curing of the resin, for subsequent cutting with a diamond disc to the dimensions required by the standards for the proposed tests. Figure 3 illustrates the flowchart of the steps involved in producing artificial rock slabs.

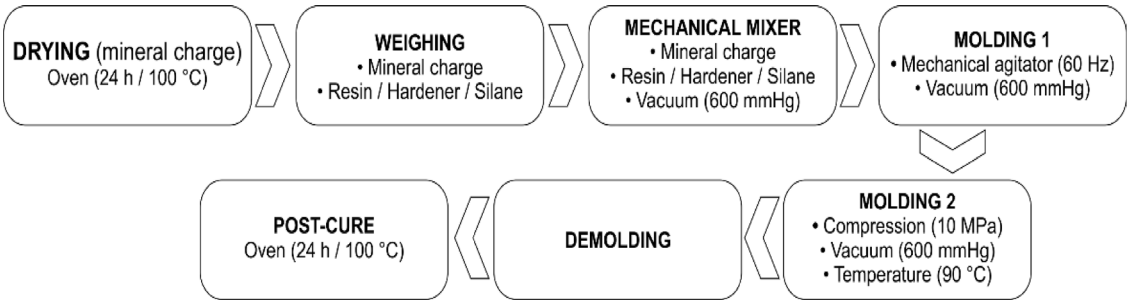

Fig. 3. Stages of manufacturing.

Legend	Resin type	Coupling agent
Epox_1	Epoxy [low viscosity + UV]	absence
Epox_1S	Epoxy [low viscosity + UV]	presence
Epox_2	Epoxy [high viscosity]	absence
Epox_2S	Epoxy [high viscosity]	presence
Poli_3	Polyester [orthophthalic]	absence
Poli_3S	Polyester [orthophthalic]	presence
Poli_4	Polyester [isophthalic]	absence
Poli_4S	Polyester [isophthalic]	presence

Table 7. Legend [artificial stones X resins].

Legend	Resin type	Coupling agent
R_Epox_1	Epoxy [low viscosity + UV]	absence
R_Epox_1S	Epoxy [low viscosity + UV]	presence
R_Epox_2	Epoxy [high viscosity]	absence
R_Epox_2S	Epoxy [high viscosity]	presence
R_Poli_3	Polyester [orthophthalic]	absence
R_Poli_3S	Polyester [orthophthalic]	presence
R_Poli_4	Polyester [isophthalic]	absence
R_Poli_4S	Polyester [isophthalic]	presence

Table 8. Legend [resins X coupling agent].

The legends for artificial rocks with 85% mineral filler and 15% resin in their compositions are presented in Table 7. The coupling agents are added in the proportion of 5% by mass, the maximum percentage indicated by the manufacturers.

Table 8 presents the captions of the test specimens produced with 100% of the resins proposed in this research. The addition of coupling agents was also present in the proportion of 5%, by mass, the maximum percentage indicated by the manufacturers.

Physical properties of the plates

To perform the physical index tests, 10 specimens measuring 50 mm x 50 mm x 10 mm were cut from the artificial rock plates. The apparent density, water absorption, and apparent porosity were determined according to ABNT/NBR 15845-2[27]. Physical tests on artificial rocks are essential for assessing the structural properties, durability, and functional performance of the material. Moreover, physical indices are critical to both quality control and compliance with technical standards.

Mechanical property (bending due to three-point loading) of artificial rock plates and resin specimens

Nine test specimens, with dimensions of $100 \times 25 \times 10$ mm, were subjected to the three-point bending test according to ABNT/NBR 15845-6[28]. The tests were conducted on an Instron 5582 universal testing machine, using a pressing speed of 0.25 mm/min, a 100 kN load cell, and a support distance of 80 mm. The bending test is one of the main mechanical tests to evaluate the mechanical properties of a material when subjected to an applied load that induces bending. This test plays a crucial role in analyzing the structural behavior of artificial rocks, enabling us to understand their strength, stiffness, and ability to withstand applied loads.

In applications such as countertops, cladding, and structural parts, the material is often subjected to loads that induce bending. The bending test reproduces this combination of tension on the bottom face and compression on the top face, providing a direct indicator of the load capacity under practical use conditions[29].

During bending, regions with pores, microcracks, or poor particle-matrix adhesion become stress concentration points, which can trigger failures. Thus, this test is particularly efficient in revealing internal heterogeneities and evaluating the effect of surface treatments on the mechanical strength of the composite[30].

For comparative purposes, a three-point bending test was performed for the four types of resin used in this research. Ten test specimens measuring $60 \times 12 \times 10$ mm were manufactured and tested as per the American standard ASTM D790-15, 2016[31] with the pressing speed of 2 mm/min, 100KN load cell, and support distance of 60 mm.

Microstructural analysis of artificial rocks

The fracture surface of specimens subjected to the bending test was analyzed using a Scanning Electron Microscope with Field Emission by Tunneling Effect (SEM-FEG) for microstructural analysis. The analysis was performed on a Tescan Mira at 20 kV of secondary electrons; the samples were metallized with a continuous gold film, ensuring the elimination of load artifacts and maximum resolution in the micrographs.

SEM allows visualization of the distribution of mineral particles within the resin matrix and the quality of the interface between them. Good adhesion reduces stress concentrations and prevents the propagation of cracks under mechanical loading, directly reflecting on properties such as flexural and compressive strength[32].

Defects such as pores and microcracks, caused by resin reaction gases or inadequate material packaging, can be detected using SEM. Porosity influences parameters such as water absorption, chemical resistance, and thermal stability. Microstructural characterization provides quantitative data on the size and distribution of these defects, allowing direct correlations with the macroscopic behavior of the composite[33].

Thermal analysis of resins with the addition of coupling agents

The thermal analysis of the resin compositions was performed using thermogravimetry (TGA) and differential scanning calorimetry (DSC). In this technique, TGA measures the variation in mass of the sample as a function of temperature. In contrast, DSC measures the heat flow associated with the thermal transitions of the sample. These analyses were performed according to the American standard ASTM D6370[34], using a TGA-SDT650 TA Instruments equipment, with a heating rate of 10 °C/min and a temperature range of 30–930 °C in a nitrogen environment.

Results and discussion

Chemical characterization of granite residue by X-ray fluorescence (XRF)

Table 9 presents, in percentage, the chemical composition of the black granite residue as determined by FRX.

The marked presence of silicon oxide (SiO2) refers to the abundance of quartz, associated mainly with muscovite and feldspar when of igneous origin. These mineralogical notes are demonstrated below with the X-ray diffractogram.

Mineralogical characterization of granite residue by X-ray diffraction (XRD)

Figure 4 illustrates the mineralogical characterization of black granite, as determined by XRD, and compares the results with those of the Joint Committee on Powder Diffraction Standards (JCPDS), now known as the International Centre for Diffraction Data (ICDD). The predominant peaks of quartz, feldspar, and mica, characteristic of magmatic rocks, are presented in the diffractogram of Fig. 4.

These results are corroborated by other research that also addresses the mineralogical characterization of black granite[35,36].

Regarding the addition of coupling agents, the peaks indicated in the diffractogram, particularly the high proportion of silica (quartz) and aluminosilicates (feldspars and micas) with surface hydroxyl groups, provide a large number of sites for silane binding. Quartz and feldspars exhibit terminal siloxane [Si–O–Si] and –Si–OH groups, which can be obtained after slight wetting, making them suitable for the condensation of silanols produced from the hydrolysis of silanes 1100 and 172. Muscovite and amphiboles present crystallite layers that expose intercalary hydroxyls; this group allows the formation of Si–O–Si bridges between the silane and the mineral skeleton[37].

About γ-Aminoprpyltriethoxysilane for epoxy resin, the –OEt groups hydrolyze to –Si–OH, which condense on the surfaces of quartz and feldspar, creating a strong Si–O–Si network. Concomitantly, the amine end [$–NH_2$] also reacts with the epoxy ring, making the C–N bond. The greater the crystalline surface area reflection of the intense peaks of quartz and feldspars, the greater the anchoring points for this silane, promoting adhesion and stress distribution[38].

SiO_2	Al_2O_3	K_2O	Na_2O	CaO	FeO
68.52	11.42	4.03	3.26	1.82	1.68
Fe_2O_3	MgO	TiO_2	P_2O_5	MnO	Fire Loss
1.22	0.71	0.30	0.12	0.05	6.87

Table 9. Chemical analysis by XRF [black granite residue].

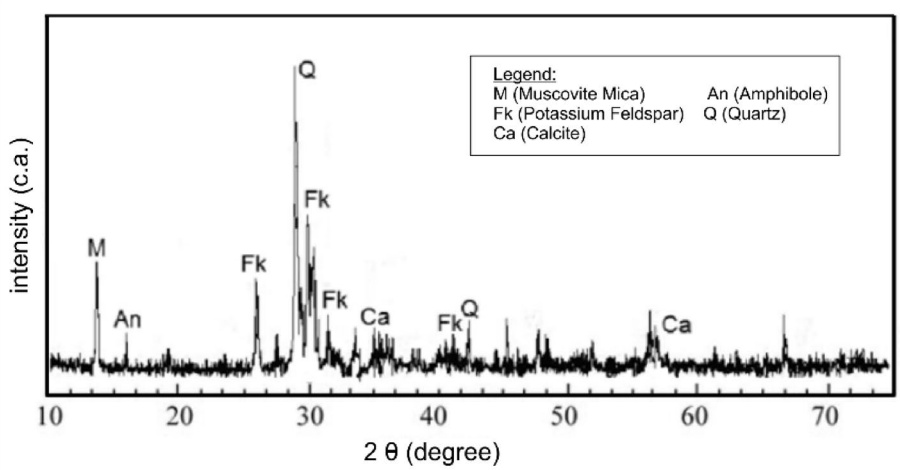

Fig. 4. Mineralogical analysis by XRF [black granite residue].

Legend	Apparent Density [g/cm³]	Apparent porosity [%]	Water Absorption [%]
Epox_1	2.172 ± 0.02	1.61 ± 0.14	1.67 ± 0.16
Epox_1S	2.194 ± 0.02	1.46 ± 0.09	0.68 ± 0.14
Epox_2	2.217 ± 0.04	1.29 ± 0.08	1.79 ± 0.11
Epox_2S	2.246 ± 0.02	0.64 ± 0.10	0.29 ± 0.08
Poli_3	2.252 ± 0.03	1.58 ± 0.07	1.89 ± 0.09
Poli_3S	2.277 ± 0.02	0.91 ± 0.09	0.79 ± 0.08
Poli_4	2.144 ± 0.03	1.36 ± 0.08	1.60 ± 0.10
Poli_4S	2.238 ± 0.02	0.53 ± 0.05	0.57 ± 0.07

Table 10. – Physical Indices.

Similarly, with 3-mercaptopropyltriethoxysilane for polyester resin, silanols anchor via Si–O–Si in the quartz/feldspar phases. The thiol end (–SH) participates in a thioene reaction with the unsaturations of the polyester, generating C–S–C bonds. Lamellar minerals such as muscovite and amphiboles with large specific surfaces favor the formation of a more uniform silane layer, enhancing the cure by offering a greater reactive interface[39].

Physical indexes

Table 10 presents the results of the physical indices of packaging #8 of the compositions, either with the addition of coupling agents, detailed in Table 2, or without the addition of coupling agents.

Physical indices in Table 8 showed optimized properties in all compositions with the inclusion of coupling agents. In poly_4S, there was an increase of approximately ± 0.213 and ± 2.37 in apparent density and apparent porosity, respectively, with variations between 1.00% and 4.38% for density and 9.32% and 61.03% for porosity. The water absorption index also demonstrated a positive change, with Epox_2S presenting the most significant improvement, from 1.19 to 0.29%, representing an 83.80% increase. The positive variations ranged from 58.20 to 83.80% in this index.

Physical indices are crucial for evaluating the quality, performance, and suitability of artificial rocks in various engineering, civil construction, interior modeling, and urban furniture applications. They also serve to predict the behavior of the material under real conditions of use. The apparent bulk density, for example, is a direct indication of the compaction of the artificial rock. The introduction of coupling agents increases the interface area between the mineral filler and the polymer matrix and, consequently, the best performance.

Figure 5 illustrates the positive results achieved after the addition of coupling agents.

Open porosity refers to the connectivity of pores, the volume of voids within the material, which directly reflects the increase or decrease in water absorption. Low porosity and water absorption are associated with high mechanical strength, less degradation (i.e., absorption of liquids and contaminants), greater durability, and resistance to corrosion and weathering[40].

Coupling agents provide the chemical adhesion that strengthens the interaction between the organic matrix and the inorganic filler. Both silanes contain alkoxysilane groups ($–Si(OC_2H_5)_3$) that hydrolyze to silanols ($–Si(OH)_3$) in the presence of moisture. These silanol groups can then react with the hydroxyl groups on the surface of the black granite filler to create siloxane bonds (–Si–O–Si–), which serve as a chemical bridge between the silane and the inorganic substrate[41].

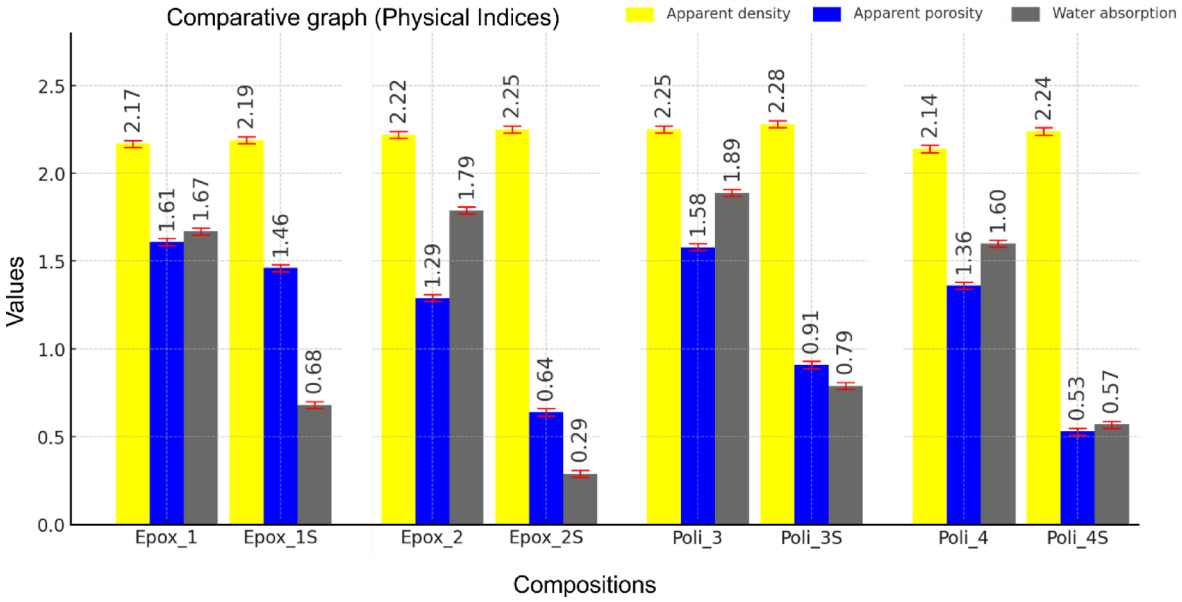

Fig. 5. Comparative graph [Physical Indices].

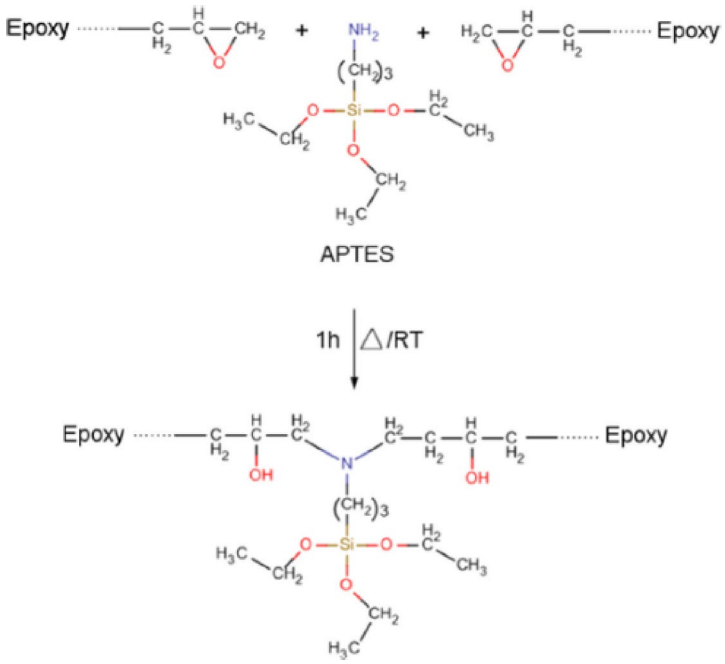

Fig. 6. Coupling reaction between γ-Aminopropyltriethoxysilane [γ-APS] and epoxy resin.

The reaction mechanism involving 3-mercaptopropyltrimethoxysilane (MPTS) and polyester resins typically centers around the thiol (SH-) group of MPTS attacking the double bonds present in the polyester systems. This interaction enables the silane to form a chemical bond with the polymer matrix. In the case of epoxy systems, the covalent bonding between the resin and treated surfaces is facilitated by the reaction between the terminal amino group of γ-APS and the epoxy groups in the epoxy resin. This bonding process is thought to enhance adhesion while improving the mechanical and chemical properties of the composites[42]. Figure 6 depicts a schematic diagram illustrating the coupling reaction between γ-Aminopropyltriethoxysilane (γ-APS) and epoxy resin[43].

compositions X coupling agent [a]		resin X coupling agent [b]	
Legend	Flexural Strength 3 points [MPa]	Legend	Flexural Strength 3 points [MPa]
Epox_1	21.53 ± 2.08	R_Epox_1	59.99 ± 2.09
Epox_1S	29.64 ± 1.19	R_Epox_1S	66.69 ± 1.48
Epox_2	34.42 ± 2.01	R_Epox_2	66.04 ± 2.06
Epox_2S	39.95 ± 1.07	R_Epox_2S	88.94 ± 2.07
Poli_3	19.91 ± 2.18	R_Poli_3	62.66 ± 2.88
Poli_3S	24.38 ± 1.76	R_Poli_3S	74.03 ± 2.36
Poli_4	27.88 ± 2.02	R_Poli_4	63.36 ± 2.00
Poli_4S	35.11 ± 1.46	R_Poli_4S	83,10 ± 1.98

Table 11. Flexural strength from three-point bending: compositions X coupling agent [a]; resin X coupling agent [b].

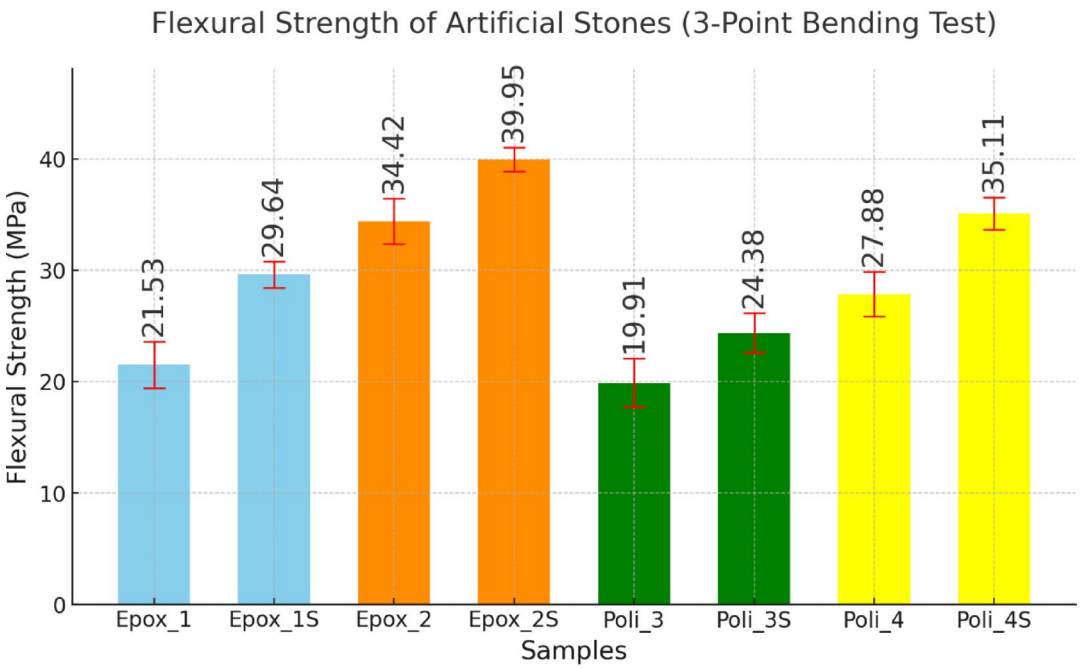

Fig. 7. Flexural strength of artificial stones [3-point bending test].

Flexural strength from three-point loading

Table 11 presents the results of the three-point loading flexural test performed on the compositions listed in Table 5, as well as the results of the test specimens with 100% of the resins and coupling agents used in this research (Table 6).

The results of the mechanical flexural test on the compositions with mineral filler and resin confirm the potential of adding coupling agents. The positive variation ranged from 16.07 to 37.67%. This occurs because the coupling agents act as "chemical bridges" between the inorganic surface of the mineral particles and the organic polymer matrix, reducing the discontinuity at the critical zone interface where mechanical failures usually occur. The result translates into more efficient stress transfer during load application[44]. Figure 7 demonstrates the positive results after the addition of coupling agents.

In the absence of the coupling agent γ-Aminopropyltriethoxysilane in epoxy resins, adhesion occurs through hydrogen bonds and van der Waals forces; with the addition of silane 1100, these interactions are replaced mainly by primary covalent bonds (Si–O–Si and C–N), increasing mechanical strength and durability[45].

Another positive characteristic that contributes to the optimization of results after the addition of silane 1100 to epoxy resins is the ability of the amine end ($–NH_2$) of the silane to open the epoxy ring, creating covalent C–N bonds between the silane and the polymer network. This generates an adsorbed film of silane chemically bonded to the resin, drastically improving adhesion and stress transfer[46].

Similar to the silane coupling agent 1100 for epoxy resin, silane 172, used for polyester resin, hydrolyzes its ethoxyl groups to silanol (–Si–OH) and condenses on the granite surface, forming Si–O–Si bridges. The thiol (–SH) end reacts via thioene addition to the remaining unsaturated double bonds in the polyester chain,

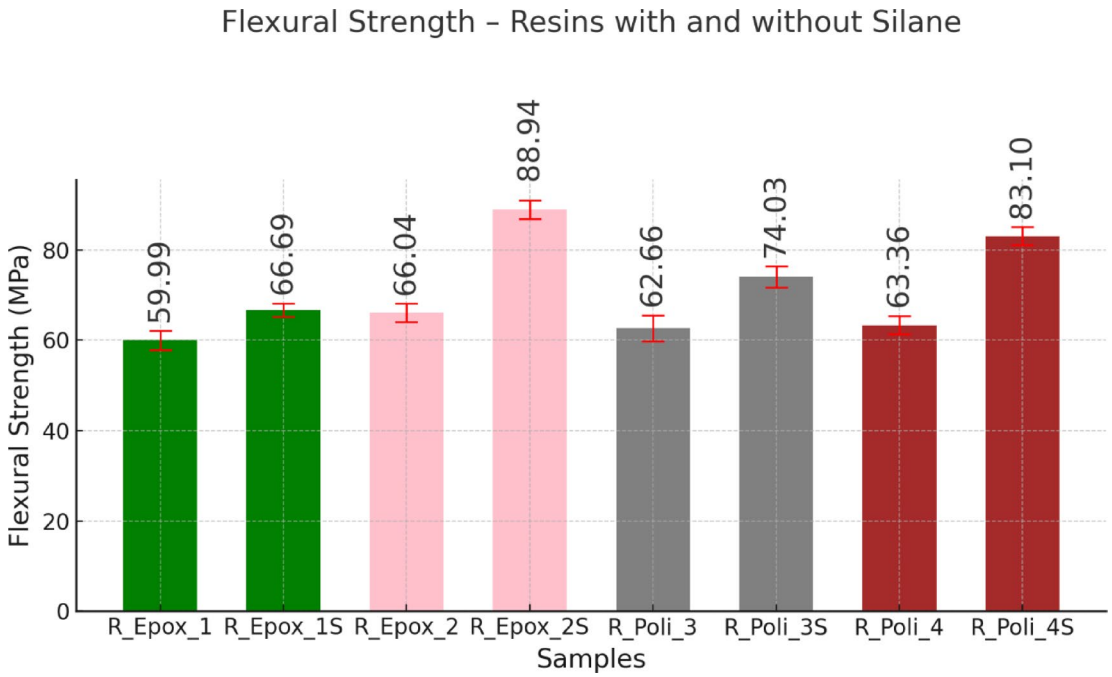

Fig. 8. Flexural Strength - Resins X Coupling Agents [3-Point Flexural Test].

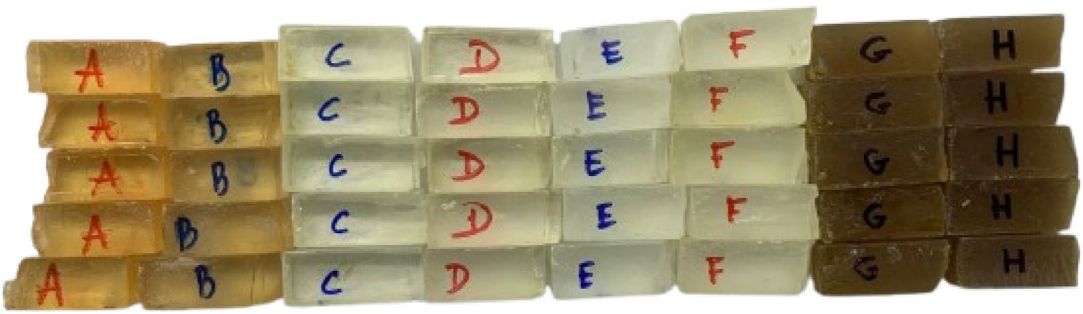

Fig. 9. Illustrates three-point bending specimens with 100% of the resins, listed in Table 6, after the flexural test.

establishing covalent C–S–C bonds between the silane and the matrix[47]. These reactions replace surface physical-chemical interactions with strong chemical bonds (Si–O–Si and C–S–C), increasing shear strength, reducing porosity, and reducing sensitivity to humidity.

Figure 8 shows the results of the mechanical flexural test on specimens with 100% resin, as listed in Table 6. The optimization of the results in the specimens with the addition of coupling agents is once again evident, primarily in the epoxy resins due to the additional cross-links, and in the polyester resins due to the copolymerization with radicals of the resin, promoting more efficient curing, lower residual stress, and reduced volume. The improvement reaches 34.68% in R_Epox_2S.

Positive results were found by Heriyanto et al.[48] mainly when the coupling agent was added to siliceous fillers [quartz, sand, and glass], presenting a greater gain in resistance due to the better chemical affinity with the silane; the improvement in flexural resistance was 50.57%, 53.29% and 81.75%, respectively.

Figure 9 – Test specimens - Resins X Coupling Agents [3-Point Bending Test]: R_Poli_4S [A]; R_Poli_4 [B]; R_Epox_1S [C]; R_Epox_1 [D]; R_Epox_2 [E]; R_Epox_2S [F]; R_Poli_3S [G]; R_Poli_3 [H]

Coupling agents enhance resin curing through new C–N and C–S bridges created by silanes, causing additional crosslinking sites, accelerating curing kinetics, and increasing the conversion of the resin's reactive functions[49]. Primary chemical coupling improves stress transfer and reduces interphase defects, resulting in composites with higher modulus, impact strength, and thermal stability[32].

Scanning electron microscopy (SEM) analysis

Figures 10, 11, 12 and 13 show the micrographs, obtained by SEM, of the fracture surfaces of the compositions that underwent the bending test.

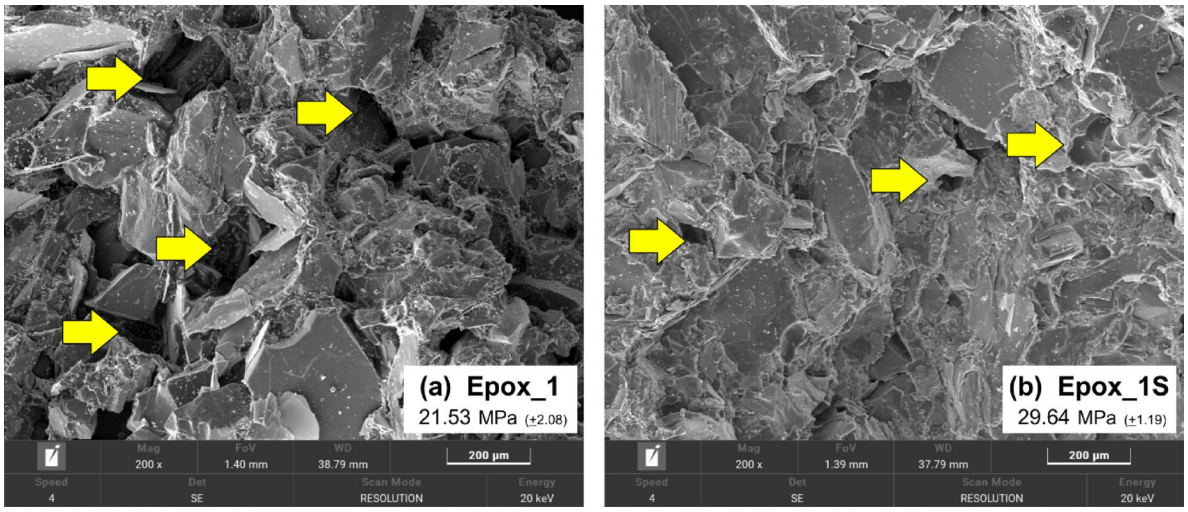

Fig. 10. Micrographs of fractures: composition [a] Epox_1 [x200] and composition [b] Epox_1S [x200].

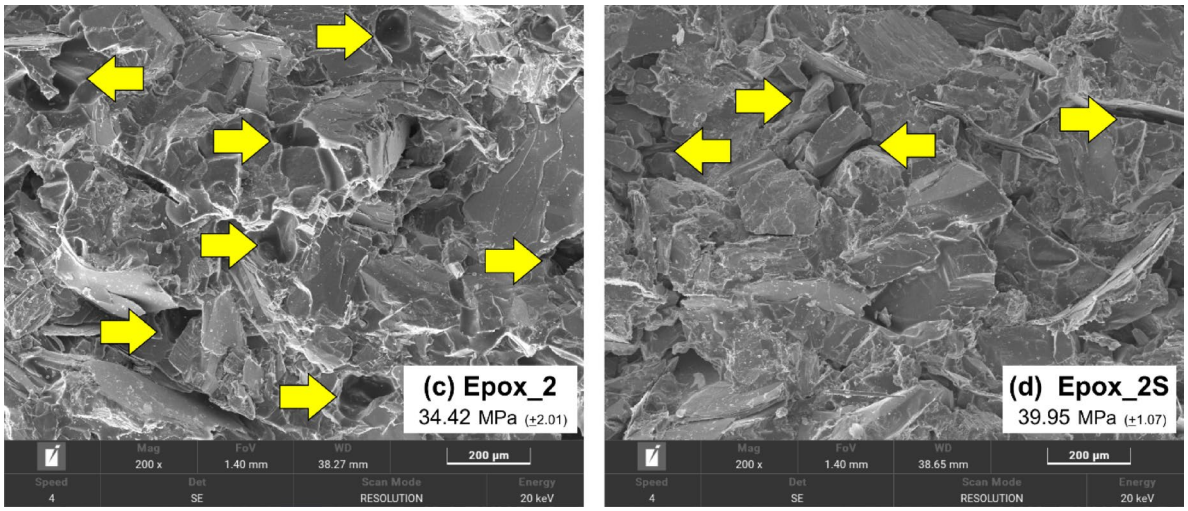

Fig. 11. Micrographs of fractures: composition [c] Epox_2 [x200] and composition [d] Epox_2S [x200].

These micrographs confirm the optimization of the mineral filler interface with the polymer matrix achieved through the use of coupling agents. The yellow arrows in the micrographs indicate the points where a failure is associated with the filler material.

After the addition of the coupling agents, these failures are mitigated not only in quantity but also in dimensions; other research corroborates the potential of silane coupling agents in improving mechanical properties[50].

SEM microscopy also revealed that, without coupling agents, the fracture surfaces exhibited porosities and adhesion failures, such as particle pull-out. However, after the addition of the agents, the fractures exhibited shear deformation (shear yielding), indicating that a greater amount of energy was absorbed before rupture, and therefore, greater mechanical resistance. Another contribution, following the addition of silane, is demonstrated by the increased efficiency in load transfer. Indeed, silane allows the mineral filler to effectively contribute to supporting stresses, since there is greater mechanical continuity between the inorganic and organic domains of the composite[48].

Thermal analysis of resins with the addition of coupling agents

The addition of coupling agents to the test specimens, with 100% of the resins present in this research, was analyzed by thermogravimetry, aiming to obtain the same positive results already found, for example, in the mechanical bending test.

Table 12 presents the comparative results after using the coupling agents, highlighting the best results in percentages after the addition of silanes.

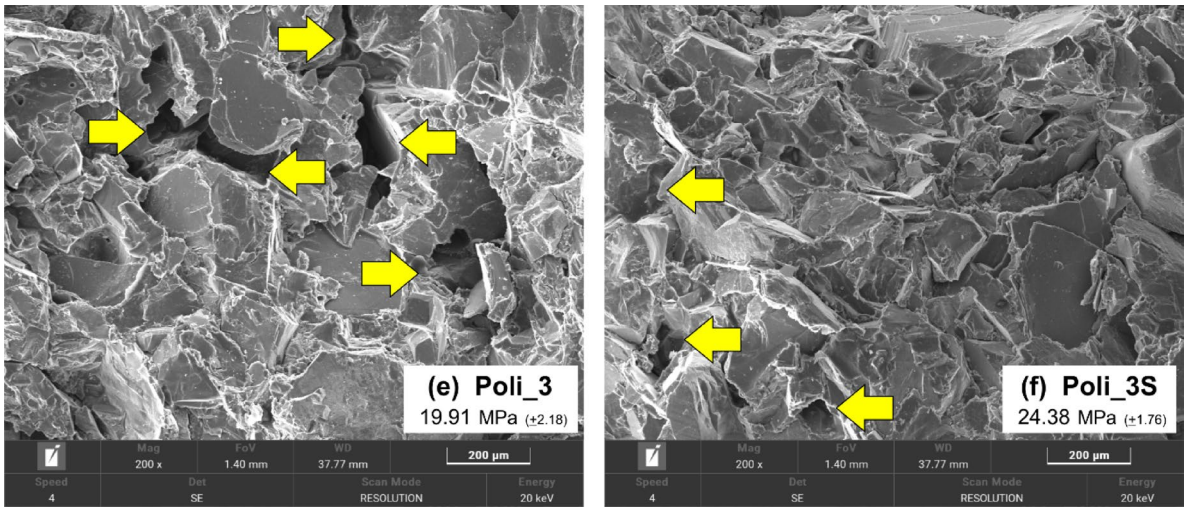

Fig. 12. Micrographs of fractures: composition [e] Poli_3 [x200] and composition [f] Poli_3S [x200].

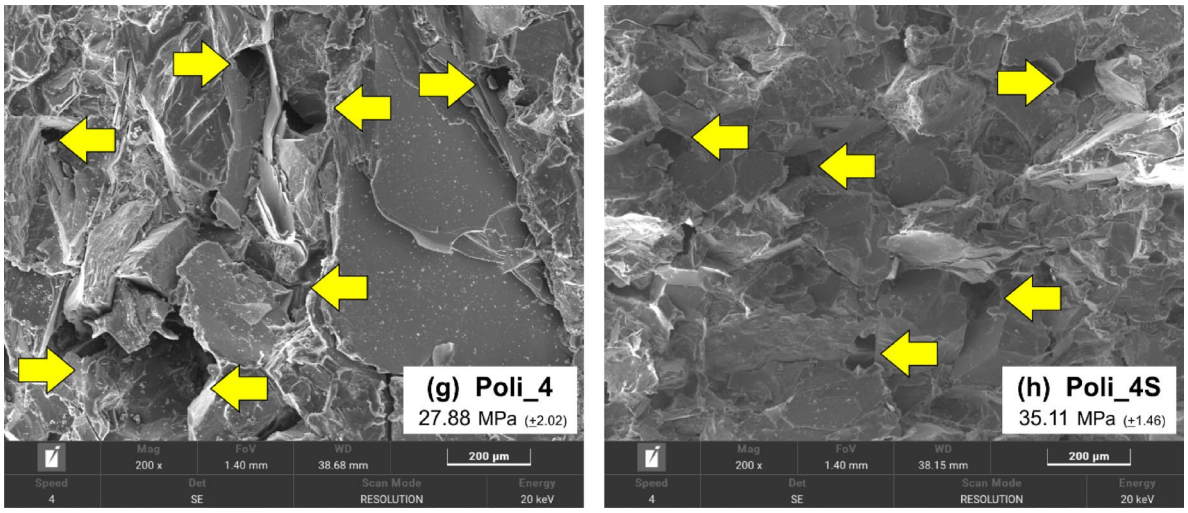

Fig. 13. Micrographs of fractures: composition [g] Poli_4 [x200] and composition [h] Poli_4S [x200].

System (without → with silane)	Mass loss without	Mass loss with	Reduction in mass loss	Characteristic T without	Characteristic T with	Residual mass without	Residual mass with
Epoxy (low viscosity) R_Epox_1 → R_Epox_1S	87.066%	61.591%	29.26%	310.3 °C	330.2 °C	12.934%	38.409%
Epoxy (high viscosity) R_Epox_2 → R_Epox_2S	90.825%	89.862%	1.06%	310.7 °C	320.5 °C	9.175%	10.138%
Polyester (orthophthalic) R_Poli_3 → R_Poli_3S	83.675%	75.962%	9.22%	345.6 °C	350.3 °C	16.325%	24.038%
Polyester (isophthalic) R_Poli_4 → R_Poli_4S	82.843%	72.824%	12.09%	345.1 °C	355.8 °C	17.157%	27.176%

Table 12. Comparison table: TGA mass loss with silane coupling agents.

Figures 14, 15, 16 and 17 show a comparison of the TGA curves for the test specimens previously listed in Table 6. It is possible to detect an increase in thermal stability and a decrease in mass loss in all resins that had the addition of coupling agents, mainly in R_Epox_1S. The addition of silane coupling agents to epoxy and polyester resin composites has been shown in several studies[51,52] to promote a significant reduction in mass loss during thermal testing.

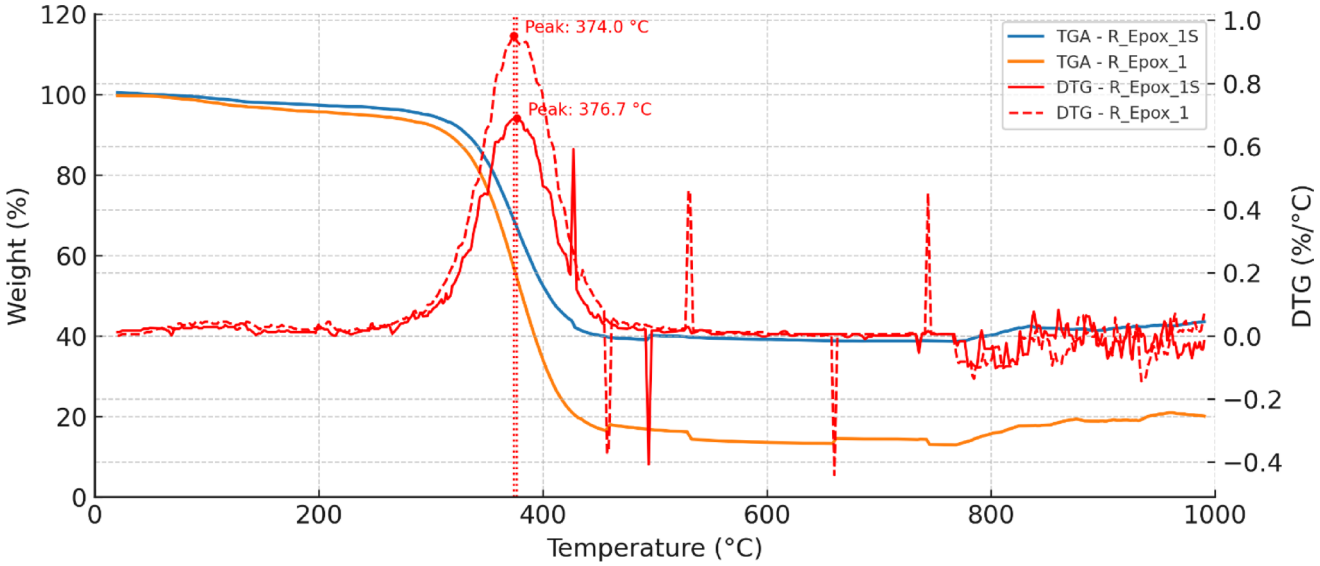

Fig. 14. Thermogravimetric curves: R_Epox_1 and R_Epox_1S.

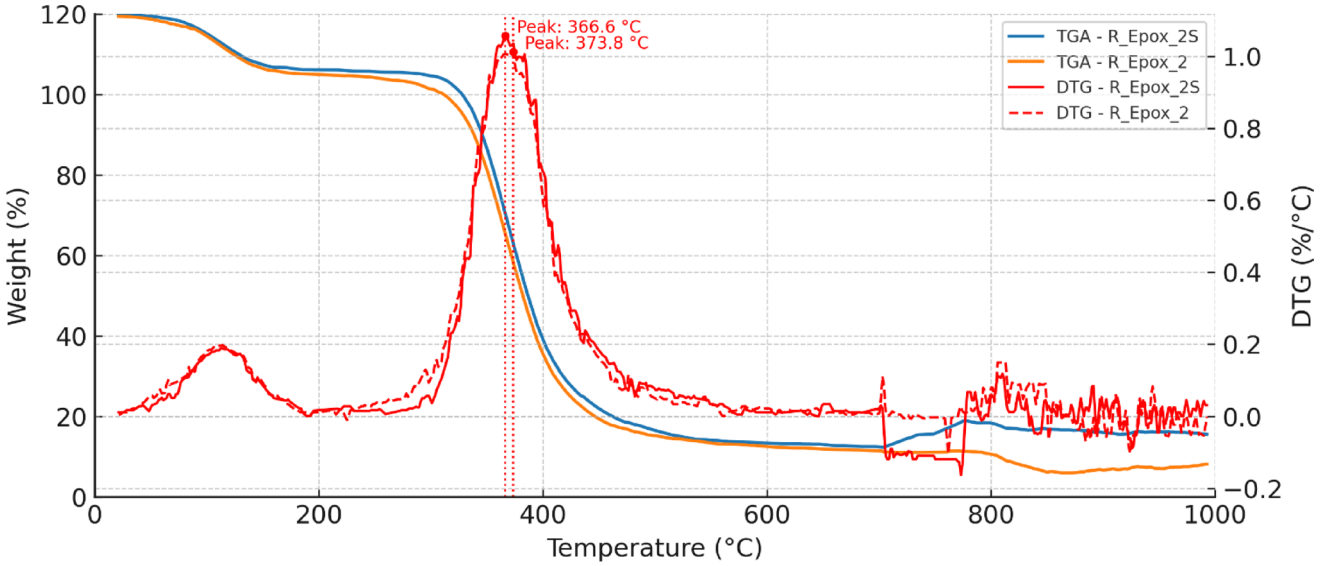

Fig. 15. Thermogravimetric curves: R_Epox_2 and R_Epox_2S.

Figure 14 shows the DTG/TGA curves of R_Epox_1 and R_Epox_1S (with coupling agent). The optimization of the results with the addition of silane is evident; although thermal stability is minimally improved, it is still present. The maximum temperature before the onset of mass loss is better in R_Epox_1S at 330.2 °C versus 310.3 °C for R_Epox_1. The mass loss after the addition of the coupling agent γ–Aminopropyltriethoxysilane is improved by 29.26%.

This improvement occurs due to the formation of a more stable chemical network, as the coupling agent γ-APS reacts with the epoxy groups of the matrix and the hydroxyls of the mineral filler, or even traces of moisture, forming Si–O–C and Si–O–Si covalent bonds, which are thermally more stable. The presence of silane strengthens the three-dimensional (3D) structure of the matrix, thereby delaying the onset of degradation and reducing the volatilization of organic fragments, which increases resistance to thermal degradation[39].

Figure 15 shows the DTG/TGA curves of R_Epox_2 and R_Epox_2S (with coupling agent). The optimization of the results follows the same trend as those obtained in Fig. 14, now using a different type of epoxy resin; the results are less notable but show improvements. Maximum thermal degradation point of 320.5 °C versus 310.7 °C, R_Epox_2S and R_Epox_2, respectively, with a 1.06% improved mass loss. This is justified by the same patterns of formation that lead to a more stable chemical network and increased molecular cohesion.

Figures 16 and 17 show that the DTG/TGA curves of the polyester resins R_Poli_3 and R_Poli_3S (with coupling agent) are orthophthalic, and R_Poli_4 and R_Poli_4S (with coupling agent) are isophthalic.

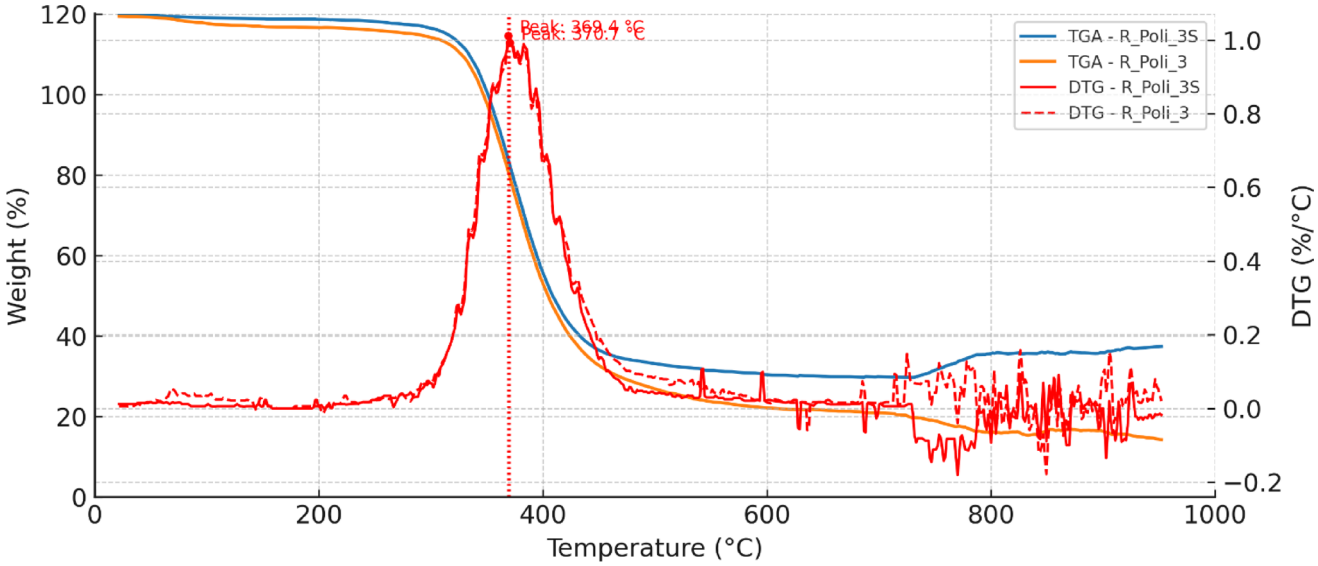

Fig. 16. Thermogravimetric curves: R_Poli_3 and R_Poli_3S.

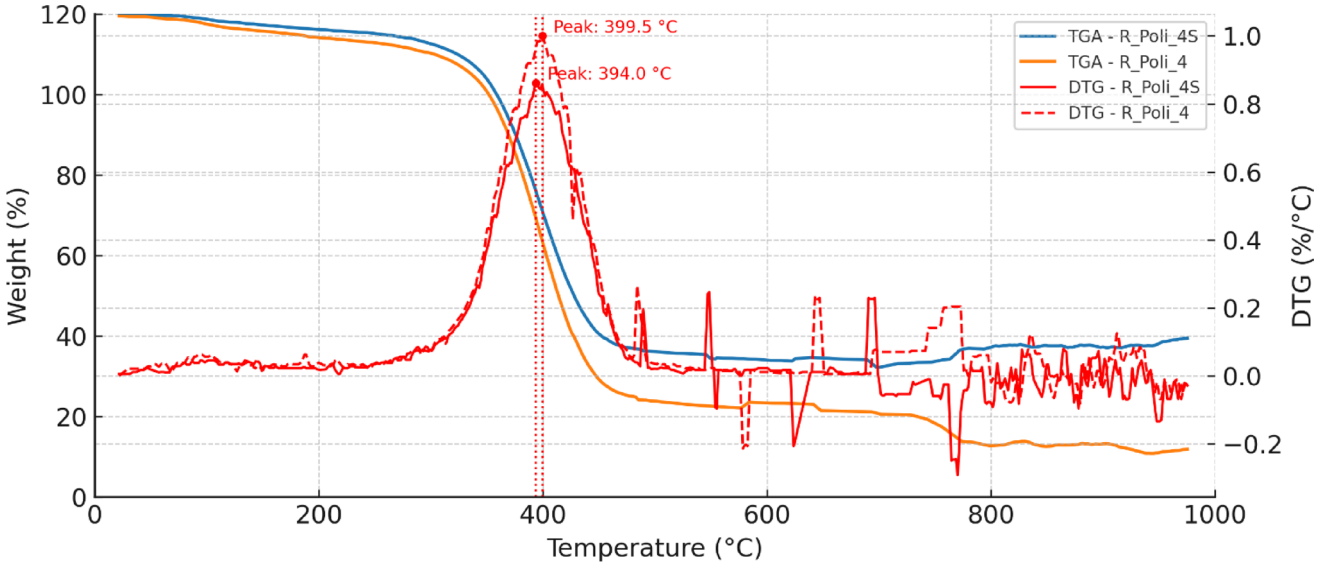

Fig. 17. Thermogravimetric curves: R_Poli_4 and R_Poli_4S.

The optimization of the results is visible and is similar between the. In the orthophthalic resin, the mass loss was optimized to 9.23% compared to 12.10% in the isophthalic resin, both with the addition of the coupling agent MPTS. Thermal stability has a slight improvement in both resins. The maximum temperature at the start of mass loss is very close, being 355.8 °C in R_Epox_4S and 350.3 °C in R_Epox_3S, both with the addition of silane. In comparison, without the addition of the coupling agent, R_Epox_4 and R_Epox_3 presented maximum temperatures of 345.1 °C and 345.6 °C, respectively.

In polyesters (orthophthalic and isophthalic), the characteristic temperatures with coupling agents were 350.3 °C (R_Poli_3S) and 355.8 °C (R_Poli_4S), whereas the neat resins presented 345.6 °C (R_Poli_3) and 345.1 °C (R_Poli_4).

These results are justified by the reaction with the polyester matrix, where the –SH (thiol) group of MPTS can react through nucleophilic addition to the unsaturated double bonds of the polyester chain (C = C), forming covalent bonds that enhance chemical crosslinking and stabilize the matrix's structure, thereby reducing its volatilization. Another point concerns the reduction of molecular mobility; the increase in the density of crosslinks and chemical interactions minimizes the degree of freedom of the chains, resulting in greater resistance to thermal degradation[48].

The difference in optimized results between polyester resins, however small, is justified by the lower molecular mobility. Indeed, the longer chains of the isophthalic resin, when crosslinked by silane, become more

immobilized, increasing the energy required to decompose the structure and, therefore, delaying the onset of degradation. Another point is the barrier to volatilization, since the silane layer forms a thin inorganic film at the interface, which acts as a barrier to the diffusion of volatile fragments during heating[53].

Other research confirms that improved TGA results are achieved when coupling agents are added. Epoxy composites modified with coupling agents exhibited an increase in the initial decomposition temperature (T_5% higher by 10–20 °C) and a higher carbon yield (char yield increased by up to 30%), demonstrating a physical/chemical barrier to volatile volatilization[54]. Polyester composites treated with coupling agents show an increase in the degradation onset temperature (T_5% increased by 8–15 °C) and a reduction in the mass loss rate in the main decomposition phase (mass loss reduced by up to 25%), reflecting better interfacial cohesion and lower diffusion of volatile products[55].

Conclusions

This research analyzed the influence of adding silane coupling agents on the composition of artificial rocks with black granite as the mineral filler and four types of resins: two epoxies and two polyesters. Based on the results, the following conclusions can be drawn:

- Porosity: reduction of up to 61.03%, from 1.29% in Epox_2 to 0.64% in Epox_2S;
- Water absorption: drop of 83.80%, from 1.79% in Epox_2 to 0.29% in Epox_2S.
- Mechanical resistance: three-point bending strength: gains ranging from 16.07% (Poli_3 X Poli_3S) to 37.67% (Poli_4 X Poli_4S);
- In the analysis of test specimens with 100% resin without the addition of mineral filler, R_Epox_2S reached 88.94 MPa, against 6.04 MPa for R_Epox_2, an optimization of 34.68%;
- Thermal stability and degradation onset temperature: increase of ~20 °C in epoxies from 310.3 °C in R_Epox_1 to 330.2 °C in R_Epox_1S; and from 345.1 °C in R_Poli_4 to 355.8 °C in R_Poli_4S;
- Total mass loss: reduction of up to 29.26% in R_Epox_1S, against R_Epox_1; and 12.10% in R_Poli_4S, against R_Poli_4;

It is concluded that the coupling agents proposed in this research work acted by hydrolyzing and chemically anchoring themselves to the granite silicate (Si–O–Si bonds), while their organofunctional ends react covalently with epoxy groups (C–N) or polyester unsaturations (C–S–C), converting secondary interactions into robust primary bonds. This justifies the use of coupling agents to optimize the adhesion and performance of artificial rocks in epoxy and polyester matrices, making them more competitive for structural, finishing, and coating applications, as well as more sustainable, by allowing greater use of mineral waste.

Data availability

All data generated or analyzed during this study are included in this published article.

Received: 21 July 2025; Accepted: 3 September 2025
Published online: 19 September 2025

References

1. ABIROCHAS. Brazilian Association of the Ornamental Rock Industry. Available: https://abirochas.com.br/ (in Portuguese).
2. CENTRO ROCHAS. Brazilian Association of Natural Rocks. (2025). Available: https://centrorochas.org.br/en/ (in Portuguese).
3. Silva, F. S., Ribeiro, C. E. G. & Rodriguez, R. J. S. Physical and mechanical characterization of artificial stone with marble calcite waste and epoxy resin. *Mater. Res.* **21** https://doi.org/10.1590/1980-5373-mr-2016-0377 (2017).
4. Bagherpor, Z., Nazari, S., Bagherzadeh, P. & Fazlavi, A. Description and effective parameters determination of the production process of fine-grained artificial stone from waste silica. *SN Appl. Sci.* **1**, 1458. https://doi.org/10.1007/s42452-019-1491-3 (2019).
5. Srinivasan, D., Ramachandran, S., Kannadasan, K., Muthukaruppan, A. & Ismail, A. A. M. Production of engineered stone from waste foundry sand using epoxy-phenalkamine binder. *Constr. Build. Mater.* **419**, 135464. https://doi.org/10.1016/j.conbuildmat.2024.135464 (2024).
6. Leng, Z., Al-Qadi, I. L. & Lahouar, S. Development and validation for in situ asphalt mixture density prediction models. *NDT E Int.* **44**, 369–375. https://doi.org/10.1016/j.ndteint.2011.03.002 (2011).
7. Alqadi, S. B., Alamleh, D., Naser Eldin, I. & Naser Eldin, H. A comparative life cycle energy and green house emissions of natural and artificial stone-manufacturing phase. *Results Eng.* **18**, 101055. https://doi.org/10.1016/j.rineng.2023.101055 (2023).
8. Zulcão, R., Calmon, J. L., Rebello, T. A. & Vieira, D. R. Life cycle assessment of the ornamental stone processing waste use in cement-based Building materials. *Constr. Build. Mater.* **257**, 119523. https://doi.org/10.1016/j.conbuildmat.2020.119523 (2020).
9. Reis, M. B. et al. Development of artificial stone through the recycling of construction and demolition waste in a polymeric matrix. (2024). https://doi.org/10.3390/su16145952
10. Santos, G. G., Crovace, M. C. & Zanotto, E. D. New engineered stones: development and characterization of mineral-glass composites. *Compos. B Eng.* **167**, 556–565. https://doi.org/10.1016/j.compositesb.2019.03.010 (2019).
11. DeArmitt, C. & Rothon, R. *Dispersants and Coupling Agents. Applied Plastics Engineering Handbook*pp. 559–575 (Elsevier, 2024). https://doi.org/10.1016/B978-0-323-88667-3.00029-1
12. Heyn, J. & Bonten, C. Influence of coupling agents on blend properties. p. 020024. (2020). https://doi.org/10.1063/1.5142939
13. Ishida, H. *Structural Gradient in the Silane Coupling Agent Layers and its Influence on the Mechanical and Physical Properties of Composites. Molecular Characterization of Composite Interfaces*pp. 25–50 (Springer US, 1985). https://doi.org/10.1007/978-1-4899-2251-9_3
14. ARKLES B. Silane Coupling Agents: Connecting Across Boundaries. Morrisville: PA: Gelest Inc; (2015). Available: https://www.gelest.com/wp-content/uploads/Silane_Coupling_Agents.pdf
15. Krishna Alla, R. Silane coupling agents-Benevolent binders in composites. Trends Biomater Artif Organs. ;31(3): 108–113. (2017). Available: http://www.sbaoi.org/tibao
16. Li, P. et al. Application of dual silane coupling Agent-Assisted Surface-Modified quartz powder in epoxy matrix for performance enhancement. *Minerals* **12**, 784. https://doi.org/10.3390/min12070784 (2022).

17. Gao, J., Mei, J., Xiong, H. & Han, X. Effect of silane coupling agents on structure and properties of carbon fiber/silicon rubber composites investigated by positron annihilation spectroscopy. *Molecules* **30**, 1658. https://doi.org/10.3390/molecules30081658 (2025).
18. ISO 12677:2011. *International Organization for Standardization. ISO 12677:2011 – Chemical Analysis of Refractory products – X-ray Fluorescence Method (XRF) – Fused cast-bead Method* (ISO, 2011).
19. ABNT NBR 7181. Brazilian Association of Technical Standards – ABNT NBR 7181: Soil – Granulometric Analysis. In: ABNT NBR 7181. (2016). Available: https://www.abntcatalogo.com.br/ (in Portuguese).
20. ABNT NBR MB 3388. Brazilian Association of Technical Standards – ABNT NBR MB 3388: Soil – Determination of the Minimum Void Index of Non-Cohesive Soils – Test Method. In: ABNT. NBR MB 3388. (1991). Available: https://www.abntcatalogo.com.br/ (in Portuguese).
21. Javorsky, J., Franchetti, M. & Zhang, H. Determining the optimal parameters of bonding Polyvinylchloride to stainless steel in automotive applications with the use of full factorial design of experiment. *CIRP J. Manuf. Sci. Technol.* **7**, 151–158. https://doi.org/10.1016/j.cirpj.2013.12.004 (2014).
22. Romli, F. I., Alias, A. N., Rafie, A. S. M. & Majid, D. L. A. A. Factorial study on the tensile strength of a Coir Fiber-Reinforced epoxy composite. *AASRI Procedia*. **3**, 242–247. https://doi.org/10.1016/j.aasri.2012.11.040 (2012).
23. de Castro, A. L. & Pandolfelli, V. C. Review: concepts of particle dispersion and packaging for the production of special concretes applied in civil construction. *Ceramic* **55**, 18–32. https://doi.org/10.1590/S0366-69132009000100003 (2009).
24. Nunes Sales Barreto, G. et al. Flexible artificial stone developed with waste tire and waste glass agglomerated by a biopolymeric resin. *J. Mater. Res. Technol.* **25**, 7417–7429. https://doi.org/10.1016/j.jmrt.2023.06.206 (2023).
25. Ribeiro, C. E. G. et al. Production of synthetic ornamental marble as a marble waste added polyester composite. *Mater. Sci. Forum*. **775–776**, 341–345. https://doi.org/10.4028/www.scientific.net/MSF.775-776.341 (2014).
26. Carvalho, E. A. S. et al. Development of epoxy matrix artificial stone incorporated with sintering residue from steelmaking industry. *Mater. Res.* **18**, 235–239. https://doi.org/10.1590/1516-1439.367514 (2015).
27. ABNT NBR15845-2. Brazilian Association of Technical Standards – ABNT NBR15845-2: Stones for Cladding. Part 2: Determination of Apparent Density, Apparent Porosity and Water Absorption. In: ABNT NBR15845-2. (2015). Available: https://www.abntcatalogo.com.br/ (in Portuguese).
28. ABNT NBR15845-6. Brazilian Association of Technical Standards – ABNT NBR 15845-6: Stones for Cladding. Part 6: Determination of the Modulus of Rupture (three-point bending). In: ABNT NBR15845-6. (2015). Available: https://www.abntcatalogo.com.br/ (in Portuguese).
29. Yap, A. U. J. & Teoh, S. H. Comparison of flexural properties of composite restoratives using the ISO and mini-flexural tests. *J. Oral Rehabil.* **30**, 171–177. https://doi.org/10.1046/j.1365-2842.2003.01004.x (2003).
30. Abdellah, M. Y., Abdelhaleem, A., Alnaser, I. A., Abdel-Jaber, G. T. & Abdal-hay, A. Flexural, compression and fracture properties of epoxy granite as a cost-effective structure materials :new machine element foundation. *AIMS Mater. Sci.* **8**, 82–98. https://doi.org/10.3934/matersci.2021006 (2021).
31. ASTM D790-15. Standard test methods for flexural properties of unreinforced and reinforced plastics and electrical insulating materials 1. (2016). https://doi.org/10.1520/D0790-15
32. Perim, T. B. et al. Characterization of artificial stone produced with blast furnace dust waste incorporated into a mixture of epoxy resin and cashew nut shell oil. *Polym. (Basel)*. **15**, 4181. https://doi.org/10.3390/polym15204181 (2023).
33. Baghloul, R., Babouri, L., Hebhoub, H., Boukhelf, F. & El Mendili, Y. Assessment of mechanical behavior and microstructure of unsaturated polyester resin composites reinforced with recycled marble waste. *Buildings* **14**, 3877. https://doi.org/10.3390/buildings14123877 (2024).
34. ASTM D6370-99. *Test Method for Rubber–Compositional Analysis by Thermogravimetry (TGA)* (ASTM International, 2014). https://doi.org/10.1520/D6370-99R14
35. Becerra, J. E. B., Costa, A. G., ACCELERATED ALTERATION TESTS FOR EVALUATION & OF SIX BRAZILIAN ORNAMENTAL GRANITES. Geonomos. (2013). https://doi.org/10.18285/geonomos.v15i2.96
36. Cavalcanti, E. B. et al. Simulated acidic weathering of black granites: an assessment using regression analysis. *Yearbook Inst. Geosci.* **46** https://doi.org/10.11137/1982-3908_2023_46_39560 (2023).
37. Masmoudi, M., Rahal, C., Abdelmouleh, M. & Abdelhedi, R. Hydrolysis process of γ-APS and characterization of silane film formed on copper in different conditions. *Appl. Surf. Sci.* **286**, 71–77. https://doi.org/10.1016/j.apsusc.2013.09.018 (2013).
38. Nakamura, M. & Ishimura, K. Synthesis and characterization of Organosilica nanoparticles prepared from 3-Mercaptopropyltrimethoxysilane as the single silica source. *J. Phys. Chem. C.* **111**, 18892–18898. https://doi.org/10.1021/jp075798o (2007).
39. Lee, M., Kim, Y., Ryu, H., Baeck, S-H. & Shim, S. E. Effects of silane coupling agent on the mechanical and thermal properties of silica/polypropylene composites. *Polym. Korea*. **41**, 599–609. https://doi.org/10.7317/pk.2017.41.4.599 (2017).
40. Demartini, T. J., da Rodríguez, C. & Silva, R. J. S. Physical and mechanical evaluation of artificial marble produced with dolomitic marble residue processed by diamond-plated bladed gang-saws. *J. Mater. Res. Technol.* **7**, 308–313. https://doi.org/10.1016/j.jmrt.2018.02.001 (2018).
41. Dow Corning Corporation. Limitless Silanes: Bonding Organic and Inorganic Materials. (2022). Available: www.dow.com/documents/26/26-2/26-2350-01-silanes-bonding-organic-inorganic-materials.pdf
42. Ji, W-G., Hu, J-M., Liu, L., Zhang, J-Q. & Cao, C-N. Water uptake of epoxy coatings modified with γ-APS silane monomer. *Prog Org. Coat.* **57**, 439–443. https://doi.org/10.1016/j.porgcoat.2006.09.025 (2006).
43. Rajan, R. et al. Modification of epoxy resin by silane-coupling agent to improve tensile properties of viscose fabric composites. *Polym. Bull.* **75**, 167–195. https://doi.org/10.1007/s00289-017-2022-2 (2018).
44. Sahai, R. S. N., Pardeshi, R. A. & Biswas, D. Effect of silane coupling agent on flexural strength and hardness of wheat straw polystyrene composites. *ASM Sci. J.* **14**, 1–6. https://doi.org/10.32802/asmscj.2020.687 (2021).
45. Ovari, T-R., Toth, T., Katona, G., Szabó, G. S. & Muresan, L. M. Epoxy coatings doped with (3-Aminopropyl)triethoxysilane-Modified silica nanoparticles for Anti-Corrosion protection of zinc. *Coatings* **13**, 1844. https://doi.org/10.3390/coatings13111844 (2023).
46. Branda, F. et al. Effect of the coupling agent (3-Aminopropyl) triethoxysilane on the structure and fire behavior of Solvent-Free One-Pot synthesized Silica-Epoxy nanocomposites. *Polym. (Basel)*. **14**, 3853. https://doi.org/10.3390/polym14183853 (2022).
47. Xie, Y., Hill, C. A. S., Xiao, Z., Militz, H. & Mai, C. Silane coupling agents used for natural fiber/polymer composites: A review. *Compos. Part. Appl. Sci. Manuf.* **41**, 806–819. https://doi.org/10.1016/j.compositesa.2010.03.005 (2010).
48. Heriyanto, P. F. & Sahajwalla, V. Effect of different waste filler and silane coupling agent on the mechanical properties of powder-resin composite. *J. Clean. Prod.* **224**, 940–956. https://doi.org/10.1016/j.jclepro.2019.03.269 (2019).
49. Šinkovec, R. & Mušič, B. Effect of organosilane coupling agents on thermal, rheological and mechanical properties of Silicate-Filled epoxy molding compound. *Materials* **13**, 177. https://doi.org/10.3390/ma13010177 (2020).
50. Urbaniak, W., Bednarek, W., Paukszta, D., Szostak, M. & Szymańska, J. The improvement in properties of polyester resin-based composites using a new type of silane coupling agent. *Polimery* **68**, 221–225. https://doi.org/10.14314/polimery.2023.4.4 (2023).
51. Chen, J., Li, B., Zhang, S. & Li, H. Effect of the presence of a silane coupling agent on reaction kinetics of cationic thermopolymerization of epoxy resin adhesive. *Coatings* **13**, 1782. https://doi.org/10.3390/coatings13101782 (2023).
52. Lee, D. S. et al. Effect of silane coupling agent on thermal stability and adhesion properties of DGEBF epoxy resin. *Polym. Korea*. **38**, 787–790. https://doi.org/10.7317/pk.2014.38.6.787 (2014).

53. Ojha, S., Bisaria, H., Mohanty, S. & Kanny, K. Mechanical performance of e-glass reinforced polyester resins (isophthalic and orthophthalic) laminate composites used in marine applications. *Proc. Institution Mech. Eng. Part. L: J. Materials: Des. Appl.* **238**, 615–626. https://doi.org/10.1177/14644207231194437 (2024).
54. Cheng, Z. et al. Thermal stability and flame retardancy of a cured trifunctional epoxy resin with the synergistic effects of silicon/titanium. *ACS Omega*. **5**, 4200–4212. https://doi.org/10.1021/acsomega.9b04050 (2020).
55. Hu, Y., Liu, Y., Zheng, S. & Kang, W. Progress in application of silane coupling agent for clay modification to flame retardant polymer. *Molecules* **29**, 4143. https://doi.org/10.3390/molecules29174143 (2024).

Acknowledgements

The authors would like to thank the laboratories and technicians of the CCT/LAMAV of the Darcy Ribeiro State University of Northern Fluminense for the opportunity and all the infrastructure provided to conduct the tests necessary for this research.

Author contributions

Conceptualization, supervision, writing—review and editing (M.B.R. and C.M.F.V.); formal analysis, investigation, writing—original draft preparation (M.B.R.; E.A.S.C.; G.C.G.D. and A.R.G.A.); writing—review and editing (C.M.F.V. and S.N.M.); funding acquisition, writing—review and editing (A.R.G.A. and C.M.F.V.)

Funding

M.B.R.'s participation was funded, respectively, by research grants from FAPERJ - E-26/201.703/2024 (300215).

Declarations

Competing interests

The authors declare no competing interests.

Additional information

Supplementary Information The online version contains supplementary material available at https://doi.org/10.1038/s41598-025-18783-4.

Correspondence and requests for materials should be addressed to A.R.G.d.A.

Reprints and permissions information is available at www.nature.com/reprints.

Publisher's note Springer Nature remains neutral with regard to jurisdictional claims in published maps and institutional affiliations.